URSI AP-RASC 2019, New Delhi, India, 09 - 15 March 2019

Sensing Radius of an Open-Ended Coaxial Probe for Dielectric Measurement of Tissues: Calculation with Relative Permittivity versus Conductivity

Alessandra La Gioia, Martin O'Halloran*, and Emily Porter
Translational Medical Device Lab, National University of Ireland Galway
Galway, Ireland
www.tmdlab.ie

Abstract

The dielectric properties of biological tissues are important parameters used in the design and optimisation of electromagnetic-based medical technologies. Typically, these parameters are measured *ex-vivo* using the open-ended coaxial probe technique. However, the accuracy of such reported dielectric data can be impacted by confounders in the measurement process. Strategies are needed to control and compensate for these confounders, which could contribute to uncertainty or error in dielectric measurements, especially for complex heterogeneous tissues. Therefore, this work examines a key source of error in the interpretation of dielectric properties. Specifically, this work investigates the sensing radius of a coaxial probe in the context of heterogeneous tissue measurements. The sensing radius is calculated for different simulated heterogeneous breast tissue samples, and the impact of using relative permittivity in the calculation of the sensing radius versus using conductivity is examined.

1. Introduction

The dielectric properties of biological tissues are vital parameters in the design and testing of electromagnetic-based medical technologies. These properties, namely, the relative permittivity and conductivity, impact the efficacy and accuracy of diagnostic and therapeutic medical devices [1]. Despite their importance, the measurement of these properties can suffer from a number of confounders, especially with heterogeneous samples [2]. Consequently, the resulting dielectric data is inconsistent for key tissues relevant to medical device development [3], [4].

This work examines one factor that may be contributing to inconsistent measurements of heterogeneous tissues. Specifically, the sensing radius of the open-ended coaxial probe is investigated. With homogeneous tissue samples, it is important that the sample radius exceeds the sensing radius of the probe, otherwise reflections from the sample edge will contaminate the measurement of the tissue properties. With heterogeneous tissue samples, the sensing radius further determines which of the tissue types present in the sample have contributed to the dielectric measurement, and in which proportions [5]. This information is especially crucial in order to accurately interpret dielectric data from heterogeneous tissues. Therefore, accurate calculation of the sensing radius is critical for dielectric studies of heterogeneous tissues.

To date, the sensing radius has been typically calculated using information on the measured relative permittivity [5]. However, the coaxial probe method also simultaneously measures the imaginary part of the complex permittivity, which can be converted into the conductivity. Most likely, the sensing radius is calculated from the relative permittivity as this parameter can be measured with higher accuracy than the conductivity [5]. As a result, it is not well understood how the sensing radius is affected by the conductivity of the tissues. Further, it is not clear how the sensing radius calculated using the relative permittivity compares to that calculated using the conductivity. Thus, this study addresses both of these gaps in knowledge.

In the next section, the study methodology is introduced. Numerical simulations are performed using a coaxial probe in contact with a range of heterogeneous tissue samples. Then, the sensing radius calculation is introduced. In Section 3, the results of the simulation are shown and the sensing radius is calculated using both the relative permittivity and the conductivity. Finally, in Section 4, a brief conclusion is provided.

2. Methodology

In this section, the study design is first presented, followed by a description of the sensing radius calculation.

2.A. Study Design

In this study, numerical simulations were designed and performed in COMSOL Multiphysics. An open-ended coaxial probe was modelled, with dimensions matched to those of the Keysight slim form probe (diameter = 2.2 mm). The slim form probe was selected as it is the most commonly used in the literature for measuring the dielectric properties of tissues [2], thanks to its small diameter [6]. Details on the simulation settings can be found in [5]. Simulations were conducted across the

2-6 GHz range, which is commonly used for microwave medical technologies [2].

In this set of simulations, heterogeneous tissue samples were composed of two tissue types: breast fat and breast gland. The dielectric properties of the tissues were obtained from the IT'IS database [7]. The heterogeneous tissue samples are designed such that they are composed of two homogeneous tissues, in a concentric arrangement, as shown in Fig. 1. In other words, an inner tissue is concentrically surrounded by an outer tissue, with the probe exactly centered on the sample. The distance from the centre of the probe to the interface between the inner and outer tissue is then varied, by varying the radius of the inner tissue (r_i). In this way, the distance can be determined at which the outer tissue is no longer detectable in the dielectric measurement. This distance is defined here as the sensing radius.

In total, 18 simulations were performed: 9 for the scenario with fat as the inner tissue (i.e., 9 different r_i) and gland as the outer tissue; and 9 for the scenario with gland as the inner tissue (i.e., 9 different r_i values) and fat as the outer tissue.

In order to calculate the sensing radius in a manner aligned to experimental studies, the complex S_{11} parameters obtained from the simulation are first converted into relative permittivity and the imaginary part of permittivity using the open–ended coaxial probe antenna model [8]. Then, the resulting relative permittivity and conductivity are used to calculate the sensing radius.

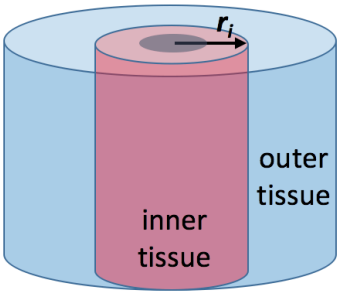

Figure 1. Diagram of the concentrically-arranged tissue samples: r_i is the radius of the inner tissue, which is variable. The probe position is indicated with the grey circle at the top of the tissue sample.

2.B. Calculation of Sensing Radius

The sensing radius is defined as the radial distance away from the centre of the probe tip at which the tissue ceases to contribute to the dielectric measurement, within the measurement uncertainty. Therefore, the measurement uncertainty must be evaluated prior to calculating the sensing radius.

In order to achieve a realistic estimate of the measurement uncertainty, experimental measurements were conducted using the Keysight slim form probe attached to a vector network analyser. The probe was calibrated using the standard three-load calibration (deionised water, short-circuit and open-circuit). Then, dielectric measurements were conducted on a standard material of known dielectric properties, i.e., 0.1 M NaCl (saline). Multiple measurements were conducted on the saline, and compared to the known properties from the literature [9]. In this way, it was determined that the measurement uncertainty in relative permittivity was 2.1% and the uncertainty in conductivity was 4.2%.

Once the measurement uncertainty has been estimated for both the relative permittivity and the conductivity, the sensing radius can be calculated. In practice, this calculation is performed by determining the percent difference between the collected dielectric data for any given sample and a reference signal, and then comparing this percent difference to the percent measurement uncertainty of the system. The reference signal is obtained when the radius of the inner tissue is large enough that only the inner tissue is measured, and effectively the measured signal is that of a measurement from a homogeneous tissue. The sensing radius is then defined as the distance at which the percent difference is equal to the measurement uncertainty. In this study, the percent difference is examined both in terms of the percent difference in relative permittivity and the percent difference in conductivity.

3. Results

First, an example of the resulting relative permittivity and conductivity trends are shown in Fig. 2, for the scenario in which the samples are composed of breast gland as the inner tissue, and breast fat as the outer tissue. The plots show data from all tissue samples in this scenario, with the radius of the inner tissue r_i varying from 0.9 mm to 3 mm. As the radius of the probe is 1.1 mm, when r_i = 0.9 mm, the inner tissue is fully contained within the size of the probe and part of the outer tissue is also in contact with the probe. From the plots, it is seen that when r_i = 0.9 mm, the contribution of the outer tissue (i.e., fat) is highest. This contribution then decreases as r_i increases. When r_i = 3 mm, the measurement is effectively that of glandular tissue; thus, this trace provides the reference signal.

Next, the calculated percent difference in relative permittivity and conductivity, each relative to their own reference signal, is plotted in Fig. 3. In Fig. 3a, the results are shown for the scenarios with fat as the inner tissue and gland as the outer tissue; and vice versa for Fig. 3b. Note that the data shown in Fig. 3b corresponds to that of Fig. 2. In each plot of Fig. 3, at each distance r_i, the percent difference shown is an average across the frequency range. The measurement uncertainty values are also shown for both relative permittivity and conductivity, as is the resulting sensing radius. While the percent differences indicate the values averaged across the frequency range, similar trends were found at each discrete frequency point by analysing single frequency data.

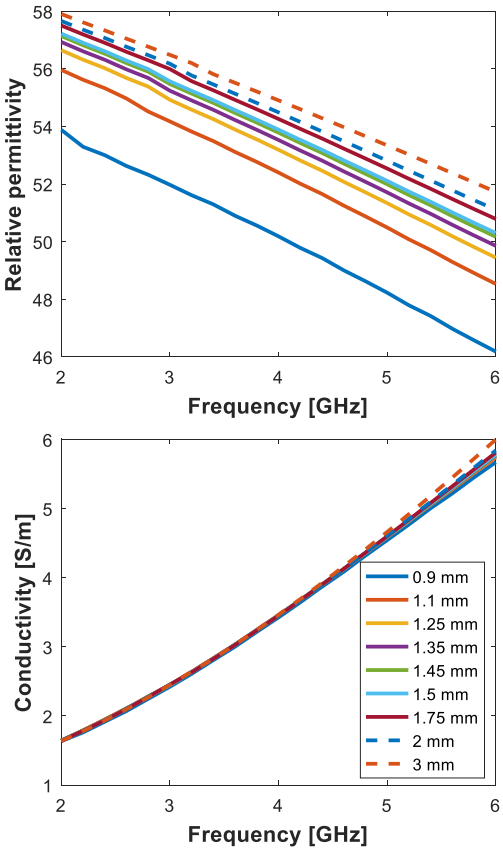

Figure 2. Relative permittivity (top) and conductivity (bottom) for the scenarios involving the concentrically heterogeneous sample composed of breast gland as the inner tissue with variable radius and breast fat as the outer tissue. The legend indicates the radius of the inner tissue (gland), r_i. As the radius of the gland tissue increases, the relative permittivity diverges from that of fat (with an average relative permittivity of 4.8) and tends toward that of gland (with an average relative permittivity of 53.5).

In Fig. 3a, the scenario consists of all samples with gland as the inner tissue and fat as the outer tissue. Thus, the sensing radius is calculated as the radius at which the outer tissue (fat) ceases to contribute to the dielectric properties, within the measurement uncertainty. Specifically, the sensing radius values refer to those averaged across the frequency range; however, similar trends were found for single frequency points. In this case, the sensing radius is found to be 1 mm for the relative permittivity-based calculation. When the sensing radius is calculated based on the conductivity, it is found to be 0.93 mm. Practically, this difference in sensing radii is small; however, if the measured complex permittivity is of interest, it is recommended to take both values into consideration. In this way, the chosen sensing radius for interpreting the dielectric data should be that of the higher value. Then, all tissues that contributed to the measurement will be included in the analysis.

Similarly, in Fig. 3b, the sensing radius for the scenario with gland as the inner tissue and fat as the outer tissue is determined to be 1.45 mm using the relative permittivity data. Calculating the sensing radius based on conductivity, however, is not possible in this scenario, as the change in conductivity is smaller than the measurement uncertainty for all acquisitions (see Fig. 2). Therefore, in this scenario, it is only the relative permittivity that is being significantly affected as the radius of the inner tissue changes. For this reason, the sensing radius calculated based on the relative permittivity can be applied to the interpretation of the complex permittivity as well.

More broadly, these results demonstrate several key points: *i*) the sensing radius varies significantly depending on the tissue type closest to the probe tip; *ii*) even in heterogeneous samples composed of the same tissue types, the sensing radius can vary based on the distribution of the tissues; and *iii*) the sensing radius is greater when a high permittivity tissue is in contact with the probe tip. Overall, this work suggests that calculation of the sensing radius should take into consideration the tissue types present in the heterogeneous sample and their relative distributions. Further, the sensing radius may be examined both in terms of the relative permittivity and the conductivity. In this case, the authors recommend that the larger sensing radius (of the two radii calculated, one from the relative permittivity and one from the conductivity) be used for interpretation of the dielectric data.

4. Conclusion

This study has examined the sensing radius of the open-ended coaxial probe, in the context of the dielectric measurement of heterogeneous tissues. Simulations were performed for concentrically heterogeneous tissue samples composed of breast gland and breast fat, while varying the radius of the heterogeneous interface. Notably, this study has examined the calculation of the sensing radius based on both the relative permittivity and the conductivity. It was found that for these tissues, the largest sensing radius of the slim form probe is only 1.45 mm. The sensing radius based on the relative permittivity and conductivity may differ, depending on the tissue properties. This underscores the importance of taking both parameters into consideration when determining the sensing radius to be used in interpreting dielectric data of heterogeneous samples. However, the sensing radius also varies based on the tissue types present in the sample and their relative distribution within the sample. Therefore, further studies are needed to comprehensively modelled these effects.

5. Acknowledgements

This research has received funding from the European Research Council under the European Union's Horizon 2020 Programme/ERC Grant Agreement BioElecPro n. 637780, Science Foundation Ireland (SFI) grant number 15/ERCS/3276, and the Hardiman Research Scholarship. This work has been developed within the framework of COST Action MyWAVE (CA17115).

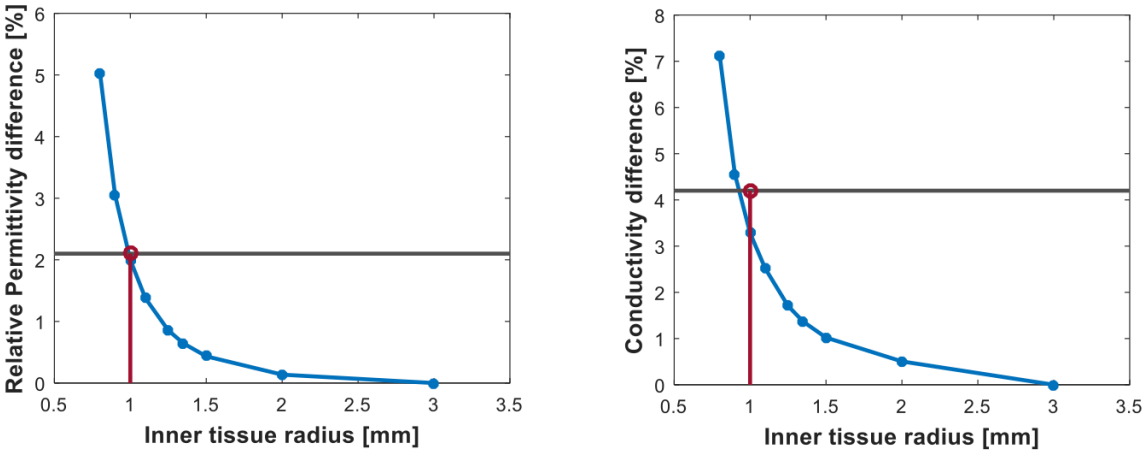

(a) Inner tissue = fat; outer tissue = gland

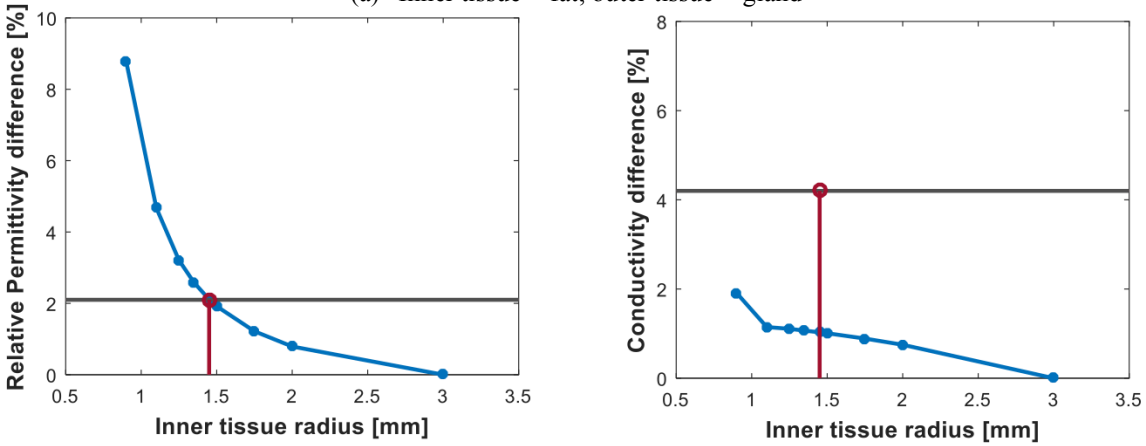

(b) Inner tissue = gland; outer tissue = fat

Figure 3. Average percent difference (across frequency) between relative permittivity (left) or conductivity (right) and the respective reference signal, plotted versus the inner tissue radius: for scenarios with fat as inner tissue and gland as outer tissue (top) and with gland as inner tissue and fat as outer tissue (bottom). The horizonal traces indicate the measurement uncertainty (2.1% for relative permittivity and 4.2% for conductivity); and the vertical red lines indicate the resulting sensing radius.

6. References

1. D. O'Loughlin *et al.*, "Microwave Breast Imaging: Clinical Advances and Remaining Challenges," *IEEE Trans. Biomed. Eng.*, **65**, 11, p. 2580–2590, 2018.

2. A. La Gioia *et al.*, "Open-Ended Coaxial Probe Technique for Dielectric Measurement of Biological Tissues: Challenges and Common Practices," *Diagnostics*, **8**, 2, pp. 1-38, 2018.

3. T. Sugitani *et al.*, "Complex permittivities of breast tumor tissues obtained from cancer surgeries," *Appl. Phys. Lett.*, **104**, 25, p. 1-5, 2014.

4. M. Lazebnik *et al.*, "A large-scale study of the ultrawideband microwave dielectric properties of normal, benign and malignant breast tissues obtained from cancer surgeries," *Phys. Med. Biol.*, **52,** 20, pp. 6093–6115, 2007.

5. A. La Gioia *et al.*, "Investigation of Histology Radius for Dielectric Characterisation of Heterogeneous Materials," *IEEE Trans. Dielectr. Insul.*, **25**, 3, pp. 1065–1080, 2018.

6. Keysight, "N1501A Dielectric Probe Kit 10 MHz to 50 GHz: Technical Overview. [Online]. Available: http://www.keysight.com/en/pd-2492144-pn-N1501A/dielectric-probe-kit," 2015.

7. P. Hasgall *et al.*, "IT'IS Database for thermal and electromagnetic parameters of biological tissues," *Version 4.0*, 2018. [Online]. Available: www.itis.ethz.ch/database.

8. D. Berube *et al.*, "A Comparative Study of Four Open-Ended Coaxial Probe Models for Permittivity Measurements of Lossy Dielectric/Biological Materials at Microwave Frequencies," *IEEE Trans. Microw. Theory Tech.*, **44**, 10, pp. 1928–1934, 1996.

9. C. Gabriel and A. Peyman, "Dielectric measurement: error analysis and assessment of uncertainty," *Phys. Med. Biol.*, **51**, 23, pp. 6033–6046, 2006.